Theoretical Study of the Electronic Spectra of Bi- and Tri-Heteronuclear Platinum Complexes

FERNANDO MENDIZABAL

Departamento de Química, Facultad de Ciencias, Universidad de Chile, Casilla 653, Santiago, Chile

ABSTRACT: The electronic structure and the spectroscopic properties of $[Pt(NH_3)_4][Au(CN)_2]_2$, $[Pt(NH_3)_4][Ag(CN)_2]_2$, $[Pt(CNCH_3)_4][Pt(CN)_4]$, and $[Pt(CNCH_3)_4][Pd(CN)_4]$ were studied at the HF, MP2, B3LYP, and PBE levels. In all the complexes, it was found that the nature of the intermetal interactions is consistent with the presence of a high-ionic contribution (90%) and a dispersion-type interaction (10%). The absorption spectra of these complexes were calculated by the single-excitation time-dependent (TD) method at the HF, B3LYP, and PBE levels. The $[Pt(NH_3)_4][M(CN)_2]_2$ (M = Au, Ag) complexes showed a $^1(d\sigma^* \rightarrow p\sigma)$ transition associated with a metal–metal charge transfer. On the other hand, the $[Pt(CNCH_3)_4][M(CN)_4]$ (M = Pt, Pd) complexes showed a $^1(d\sigma^* \rightarrow \pi^*)$ transition associated with a metal-to-metal and ligand charge transfer. The values obtained theoretically are in agreement with the experimental range.

Key words: heavy atoms; electronic spectra; time-dependent

Introduction

In recent years, the bonding interaction between closed-shell metal atoms has been widely studied from the theoretical and experimental viewpoints [1, 2]. Among the heavy metal atoms gold–gold interactions (aurophilicity) have received the greatest attention. Other metals (Ag(I), Pt(II), Pd(II), etc.) containing heterometallic systems in which short closed-shell metal–metal interactions are present (metallophilicity) can also be found in recent articles [3–6]. For example, Au^I–Pd^{II} (d^{10}–d^8) [7], Au^I–Ag^I (d^{10}–d^{10}) [8], Au^I–Cu^I (d^{10}–d^{10}) [8], and Au^I–Tl^I (d^{10}–s^2)[9–11] interactions have been described theoretically using correlated methods, and it has been shown that the metallophilic interactions arise from dispersion-type correlation effects (van der Waals) and charge transfer contributions [11].

On the other hand, the closed-shell d^8 ions such as platinum(II), also shown to interact through Pt–M interactions, provide an additional electro-

Correspondence to: F. Mendizabal; e-mail: hagua@chile.cl
Contract grant sponsor: Fondecyt (Conicyt-Chile).
Contract grant number: 1060044.

static attraction [12]. Such interactions are seen in the extended chain structures present in tri- and dimeric complexes such as oligomers $[Pt(NH_3)_4][M(CN)_2]_2$ (M = Au, Ag) and $[Pt(CNCH_3)_4][Pt(CN)_4]$ (M = Pt, Pd) [13, 14]. Experimentally, the d^8 Pt(II) complexes that stack in the solid state show a strong $^1(d\sigma^* \rightarrow p\sigma)$ UV–visible transition of the metal-to-metal or ligand charge transfer (MMLCT) type. The increase in energy of the $^1(d\sigma^* \rightarrow p\sigma)$ or $^1(d\sigma^* \rightarrow \pi^*)$ transition depends on the type of interaction and the metal–metal distance [13, 14].

The complexes studied here show evidence of metallophilic interactions with a strong ionic contribution. The optical properties of the complexes can be calculated from density functional theory (DFT) with the time-dependent (DFT-TD) approach. Several articles have shown an excellent association with experimental absorption and emission spectra [15–17]. Lately, we have studied the electronic structure and the spectroscopic properties of $[M(CN)_2]_n^{-n}$ (M = Au(I), Ag(I); n = 1–3) using DFT at the B3LYP level [18]. The di- and trinuclear models show an $^1(nd\sigma^* \rightarrow (n+1)p\sigma)$ transition associated with a metal–metal charge transfer, which is strongly interrelated with the gold–gold and silver–silver contacts. A variation of the previous systems is proposed here which includes the effect of a metal with a d^8 (Pt (II)) electronic configuration.

The objective of this work is to study theoretically the interaction energies and excitation spectra of complexes of type $[Pt(NH_3)_4][M(CN)_2]_2$ (M = Au, Ag) and $[Pt(CNCH_3)_4][M(CN)_4]$ (M = Pt, Pd) at the HF, MP2, B3LYP, and PBE levels. So far there has been no systematic research done on these models.

Models and Methods

Models **1–4** used in our study are depicted in Figure 1. For Models **3** and **4**, a simplified system of the experimental structures with the general formula $[Pt(CN\text{-}iso\text{-}C_3H_7)_4][M(CN)_4]$ (M = Pt, Pd) is used [14]. We have replaced the CN-iso-C_3H_7 ligand by CN—CH_3 due to the large computational effort. The geometries were fully optimized at the scalar relativistic HF, MP2, B3LYP, and PBE (Perdew-Burke-Ernzerhof) [19] levels in the gas phase for each fragment. The main geometric parameters are shown in Table I. We used these geometries to study the metal–metal intermolecular interactions. The metal–metal interaction energy $V(R_e)$ and geometric equilibrium (R_e) of the complexes were obtained with a counterpoise correction for the basis-set superposition error (BSSE). The optimized interaction energies ($V(R_e)$) and metal–metal distances (R_e) for the complexes are shown in Table II.

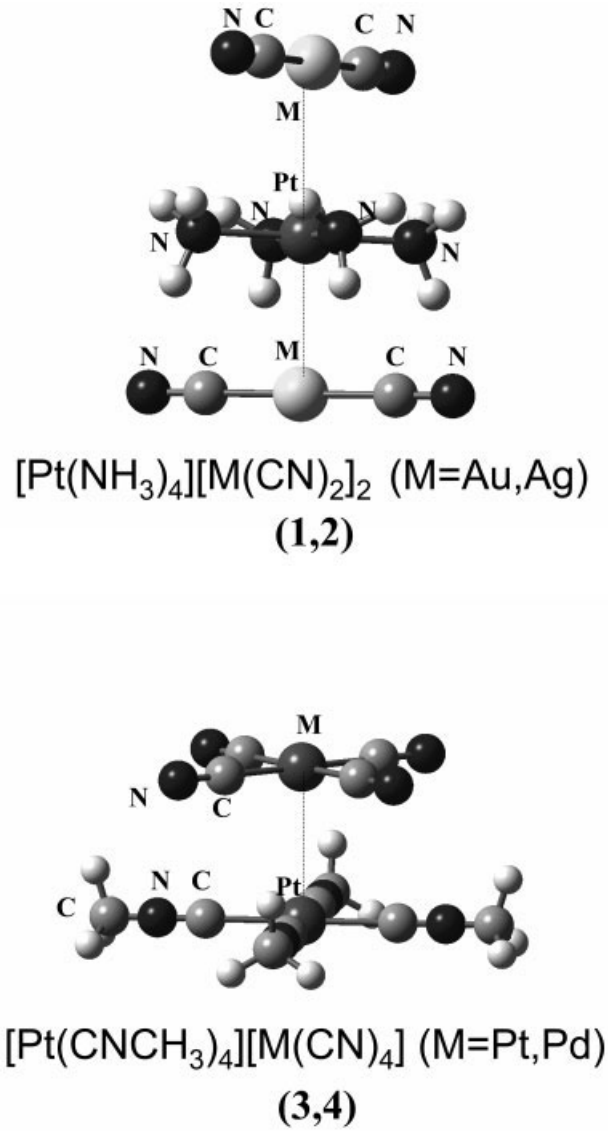

FIGURE 1. The $[Pt(NH_3)_4][Au(CN)_2]_2$ (**1**), $[Pt(NH_3)_4][Ag(CN)_2]_2$ (**2**), $[Pt(CNCH_3)_4][Pt(CN)_4]$ (**3**), and $[Pt(CNCH_3)_4][Pd(CN)_4]$ (**4**) models.

Single-point calculations of these geometries were simulated to study the excitation spectra by HF, B3LYP, and PBE (DFT). The excitation energy was obtained using the time-dependent perturbation theory approach (TD) [20, 21], which is based on the random-phase approximation (RPA) method [21]. The TD approach provides an alternative to

TABLE I

Main geometric parameters of the monomers used.

Monomer	Method	M–C	C–N	∠M–C–N
$[Au(CN)_2]^-$	HF	204.7	114.2	180.0
	MP2	197.1	118.5	180.0
	B3LYP	200.3	116.6	180.0
	PBE	198.7	117.8	180.0
$[Ag(CN)_2]^-$	HF	214.5	114.2	180.0
	MP2	201.6	118.5	180.0
	B3LYP	205.2	116.7	180.0
	PBE	202.8	117.8	180.0
$[Pt(CN)_4]^{-2}$	HF	205.4	114.4	180.0
	MP2	197.5	119.1	180.0
	B3LYP	201.9	117.1	180.0
	PBE	200.3	118.3	180.0
$[Pd(CN)_4]^{-2}$	HF	201.2	114.5	180.0
	MP2	192.8	119.1	180.0
	B3LYP	197.5	117.1	180.0
	PBE	196.2	118.4	180.0

Monomer	Method	Pt–N	N–H	∠Pt–N–H
$[Pt(NH_3)_4]^{+2}$	HF	212.3	101.2	113.2
	MP2	208.1	102.6	113.1
	B3LYP	210.8	102.9	112.9
	PBE	209.8	103.5	112.9

Monomer	Method	Pt–C	C–N	C–N	C–H	∠H–C–N
$[Pt(CNCH_3)_4]^{+2}$	HF	205.0	112.7	144.7	108.4	107.9
	MP2	196.4	116.7	144.3	109.5	108.1
	B3LYP	200.8	115.2	143.9	109.8	108.5
	PBE	199.0	116.4	142.5	110.7	108.9

Distances in pm and angles in degrees.

computationally demanding multireference configuration interaction methods in the study of excited-states. The TD calculations do not evaluate the spin-orbit splitting, the values are averaged.

Calculations using the Gaussian 03 package were done [22]. The 19 valence-electrons (VE) of Au and Ag, 18 VE of Pt, and the Pd quasi-relativistic (QR) pseudo-potential (PP) of Andrae et al. [23] were employed. We used two *f*-type polarization functions on gold (α_f = 0.20, 1.19), silver (α_f = 0.22, 1.72), platinum (α_f = 0.70, 0.14), and palladium (α_f = 2.203, 0.621) [14]. Also, the C and N atoms were treated through PPs, using double-zeta basis sets with the addition of one *d*-type polarization function [24]. For the H atom, a double-zeta basis set plus one *p*-type polarization function was used [25].

Results and Discussion

MOLECULAR GEOMETRY

Table II summarizes the metal–metal interaction energies and equilibrium distances for Models **1–4**. The theoretical results are in agreement with the experimental data. The metal–metal distances are overestimated for all models, though the experimental trend is maintained. Concerning the metal–metal distance and the interaction energy, it is noteworthy that the electronic correlation effects play an important role in the stability of the systems.

In general, metal–metal distances at the HF level are longer than those obtained by other methods (MP2, B3LYP, and PBE). The interaction energies

TABLE II

The optimized interaction energies and metal–metal distances for the complexes.

System	Method	M–M	ΔE	F	ν
$[Pt(NH_3)_4][Au(CN)_2]_2$ (1)	HF	314.9	−0.42752	85.60	92
	MP2	293.6	−0.47734	140.25	118
	B3LYP	300.9	−0.44699	109.67	104
	PBE	294.7	−0.36662	122.83	111
	Exp.	328.0			
$[Pt(NH_3)_4][Ag(CN)_2]_2$ (2)	HF	307.7	−0.42530	87.96	102
	MP2	290.4	−0.47386	136.54	127
	B3LYP	296.4	−0.44957	111.21	115
	PBE	290.2	−0.37124	122.92	121
	Exp.	325.0			
$[Pt(CNCH_3)_4][Pt(CN)_4]$ (3)	HF	306.5	−0.38579	70.56	86
	MP2	283.7	−0.43342	127.42	115
	B3LYP	296.7	−0.40286	85.68	94
	PBE	286.2	−0.43509	110.18	107
	Exp.	316.0			
$[Pt(CNCH_3)_4][Pd(CN)_4]$ (4)	HF	305.1	−0.38488	65.78	91
	MP2	282.4	−0.42592	114.07	120
	B3LYP	293.8	−0.40029	82.47	102
	PBE	271.8	−0.46411	123.25	125
	Exp.	317.0			

Optimized M–M distances (R_e), in pm; interaction energies (ΔE), with counterpoise correction, in kJ/mol; force constant (F) M–M, in Nm^{-1}; harmonic frequency (ν), in cm^{-1}.

TABLE III

NBO analysis of the PBE density for the models studied.

System	Atom	Natural	Natural electron configuration
$[Pt(NH_3)_4][Au(CN)_2]_2$(1)	Au	0.33535	$6s^{1.02}\ 5d^{9.63}\ 6p^{0.01}\ 7p^{0.01}$
	Pt	0.69344	$6s^{0.5}\ 5d^{8.71}\ 6p^{0.01}\ 5f^{0.01}\ 6d^{0.01}\ 7p^{0.01}$
	N	−1.00004	$2s^{1.49}\ 2p^{4.50}\ 3p^{0.01}$
	C	−0.18819	$2s^{1.23}\ 2p^{2.90}\ 3s^{0.03}\ 3p^{0.03}\ 3d^{0.01}$
	N	−0.45163	$2s^{1.58}\ 2p^{3.86}\ 3s^{0.01}$
$[Pt(NH_3)_4][Ag(CN)_2]_2$ (2)	Ag	0.45883	$5s^{0.75}\ 4d^{9.78}\ 5p^{0.01}$
	Pt	0.67620	$6s^{0.55}\ 5d^{8.71}\ 6p^{0.01}\ 5f^{0.01}\ 6d^{0.01}$
	N	−1.00084	$2s^{1.49}\ 2p^{4.50}\ 3p^{0.01}$
	C	−0.23675	$2s^{1.30}\ 2p^{2.87}\ 3s^{0.03}\ 3p^{0.03}\ 3d^{0.01}$
	N	−0.46284	$2s^{1.58}\ 2p^{3.87}\ 3s^{0.01}$
$[Pt(CNCH_3)_4][Pt(CN)_4]$ (3)	Pt	0.34444	$6s^{0.70}\ 5d^{8.89}\ 6p^{0.03}\ 5f^{0.01}\ 6d^{0.01}\ 7p^{0.01}$
	C	−0.02691	$2s^{1.17}\ 2p^{2.80}\ 3s^{0.03}\ 3p^{0.03}\ 3d^{0.01}$
	N	−0.50984	$2s^{1.58}\ 2p^{3.92}\ 3s^{0.01}$
	Pt	0.45794	$6s^{0.65}\ 5d^{8.85}\ 6p^{0.01}\ 6d^{0.01}\ 8s^{0.01}$
	C	0.35778	$2s^{1.14}\ 2p^{2.46}\ 3s^{0.01}\ 3p^{0.02}\ 3d^{0.01}$
	N	−0.36952	$2s^{1.21}\ 2p^{4.15}\ 3s^{0.01}\ 3p^{0.01}$
	C	−0.38500	$2s^{1.11}\ 2p^{3.27}\ 3d^{0.01}$
$[Pt(CNCH_3)_4][Pd(CN)_4]$ (4)	Pd	0.29709	$5s^{0.57}\ 4d^{9.11}\ 5p^{0.03}\ 5d^{0.01}\ 6p^{0.01}\ 6d^{0.01}\ 7p^{0.01}$
	C	−0.01227	$2s^{1.20}\ 2p^{2.75}\ 3s^{0.03}\ 3p^{0.03}\ 3d^{0.01}$
	N	−0.51638	$2s^{1.58}\ 2p^{3.92}\ 3s^{0.01}$
	Pt	0.45090	$6s^{0.65}\ 5d^{8.85}\ 6p^{0.01}\ 6d^{0.01}\ 7p^{0.01}\ 8s^{0.01}$
	C	0.35837	$2s^{1.14}\ 2p^{2.46}\ 3s^{0.01}\ 3p^{0.02}\ 3d^{0.01}$
	N	−0.36541	$2s^{1.21}\ 2p^{4.15}\ 3s^{0.01}\ 3p^{0.01}$
	C	−0.38513	$2s^{1.11}\ 2p^{3.27}\ 3d^{0.01}$

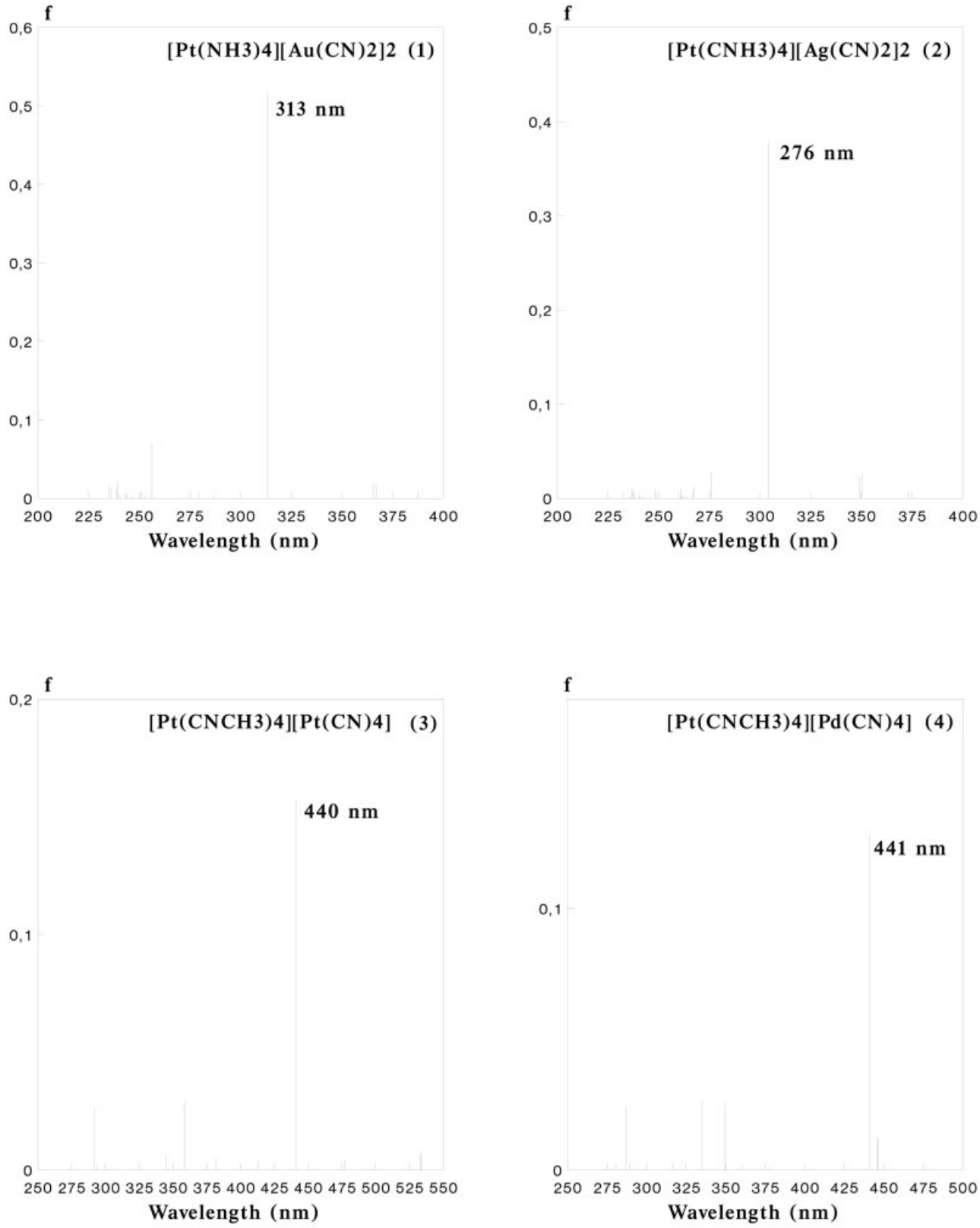

FIGURE 2. Calculated electronic PBE spectra of all complexes.

TABLE IV

TD-HF and TD-DFT singlet-excitation calculations for the models.

System	Method	λ_{calc} (nm)	f [a]	Contribution[b]	Transition type
$[Pt(NH_3)_4][Au(CN)_2]_2$ (1)	HF	193	1.0162	$62a_1 \rightarrow 68a_1$ (80)	MMCT ($d\sigma^* \rightarrow p\sigma$)
	B3LYP	265	0.6364	$62a_1 \rightarrow 67a_1$ (89)	MMCT ($d\sigma^* \rightarrow p\sigma$)
	PBE	313	0.5176	$62a_1 \rightarrow 67a_1$ (85)	MMCT ($d\sigma^* \rightarrow p\sigma$)
	Exp.	380			
$[Pt(NH_3)_4][Ag(CN)_2]_2$ (2)	HF	180	0.8652	$62a_1 \rightarrow 69a_1$ (70)	MMCT ($d\sigma^* \rightarrow p\sigma$)
	B3LYP	254	0.5516	$62a_1 \rightarrow 67a_1$ (89)	MMCT ($d\sigma^* \rightarrow p\sigma$)
	PBE	304	0.3778	$62a_1 \rightarrow 67a_1$ (80)	MMCT ($d\sigma^* \rightarrow p\sigma$)
$[Pt(CNCH_3)_4][Pt(CN)_4]$ (3)	HF	245	0.3935	$68a_1 \rightarrow 69a_1$ (75)	MMLCT ($d\sigma^* \rightarrow \pi^*$)
	B3LYP	388	0.2300	$68a_1 \rightarrow 69a_1$ (80)	MMLCT ($d\sigma^* \rightarrow \pi^*$)
	PBE	440	0.1575	$68a_1 \rightarrow 69a_1$ (80)	MMLCT ($d\sigma^* \rightarrow \pi^*$)
	Exp.	593			
$[Pt(CNCH_3)_4][Pd(CN)_4]$ (4)	HF	207	0.3358	$68a_1 \rightarrow 69a_1$ (39)	MMLCT ($d\sigma^* \rightarrow \pi^*$)
	B3LYP	381	0.1830	$68a_1 \rightarrow 69a_1$ (85)	MMLCT ($d\sigma^* \rightarrow \pi^*$)
	PBE	441	0.1278	$68a_1 \rightarrow 69a_1$ (76)	MMLCT ($d\sigma^* \rightarrow \pi^*$)

[a] Oscillator strength.
[b] Values are $|coeff.|^2 \times 100$.

are in the range of ionic interactions. When we take the HF level as reference, in all the models the interaction energy at the MP2 level consists of 90% ionic interaction and 10% van der Waals interactions. Thus, we are assuming that the ionic interaction is responsible for the attractive behavior at the HF level. This large magnitude occurs because the fragments that give rise to the models show a high formal charge.

The natural bond orbital (NBO) population analysis of the complexes is shown in Table III. This analysis is based on the PBE density. A large charge is seen on the metallic centers. This confirms the principal ionic contribution.

The energy differences between HF and MP2 in Models **1–4** are 146 kJ/mol (**1**, Pt-Au pair), 69 kJ/mol (**2**, Pt-Ag pair), 139 kJ/mol (**3**, Pt-Pt pair), and 121 kJ/mol (**4**, Pt-Pd pair). For Models **1** and **2**, these values are within the range of magnitude of dispersion-type van der Waals interactions with charge transfer, with the silver system presenting a smaller interaction. On the other hand, Models **3** and **4** show a high interaction energy beyond the limit of dispersion with charge transfer. We think that this is an overestimation of the method used (MP2), since the metal–metal distances are shorter than the experimental values. This contributes to a greater interaction energy. The energy magnitudes confirm that the PtPt (**3**) complex is more stable than the PtPd (**4**) complex, which is in agreement with the experiments [25].

TIME-DEPENDENT, HF AND DFT CALCULATIONS

We calculated the allowed spin-singlet transition for these systems, based on the ground state structures of Models **1–4** at the HF, PBE, and B3LYP levels. The objective was to evaluate the electronic structure of the excited state by direct electronic excitations. Only singlet–singlet transitions were considered in these QR calculations. The allowed transitions are shown in Figure 2 and are listed in Table IV. The active molecular orbitals in electronic transitions at the PBE level are shown in Figures 3 and 4.

$[Pt(NH_3)_4][M(CN)_2]_2$ (M = Au, Ag) (1 and 2)

The gold complex shows an experimental absorption spectra with a characteristic band at 380 nm [14]. On the other hand, there are no reports of the absorption spectra of the silver complex.

The theoretical calculations are described in Table IV. The calculated spectra show a principal transition that changes depending on the methodology used. We can observe a red shift when we go from HF to PBE. The latter method approached the experimental value. The deviation may be due to the fact that the compounds are found in stack solid state experimentally. The complexes showed oligomer structures. Thus, the agreement is at semiquantitative level. This effect was seen theoretically in the $[Au_3(MeN{=}COMe)_3]_n$ (n = 2–4) [26]. The

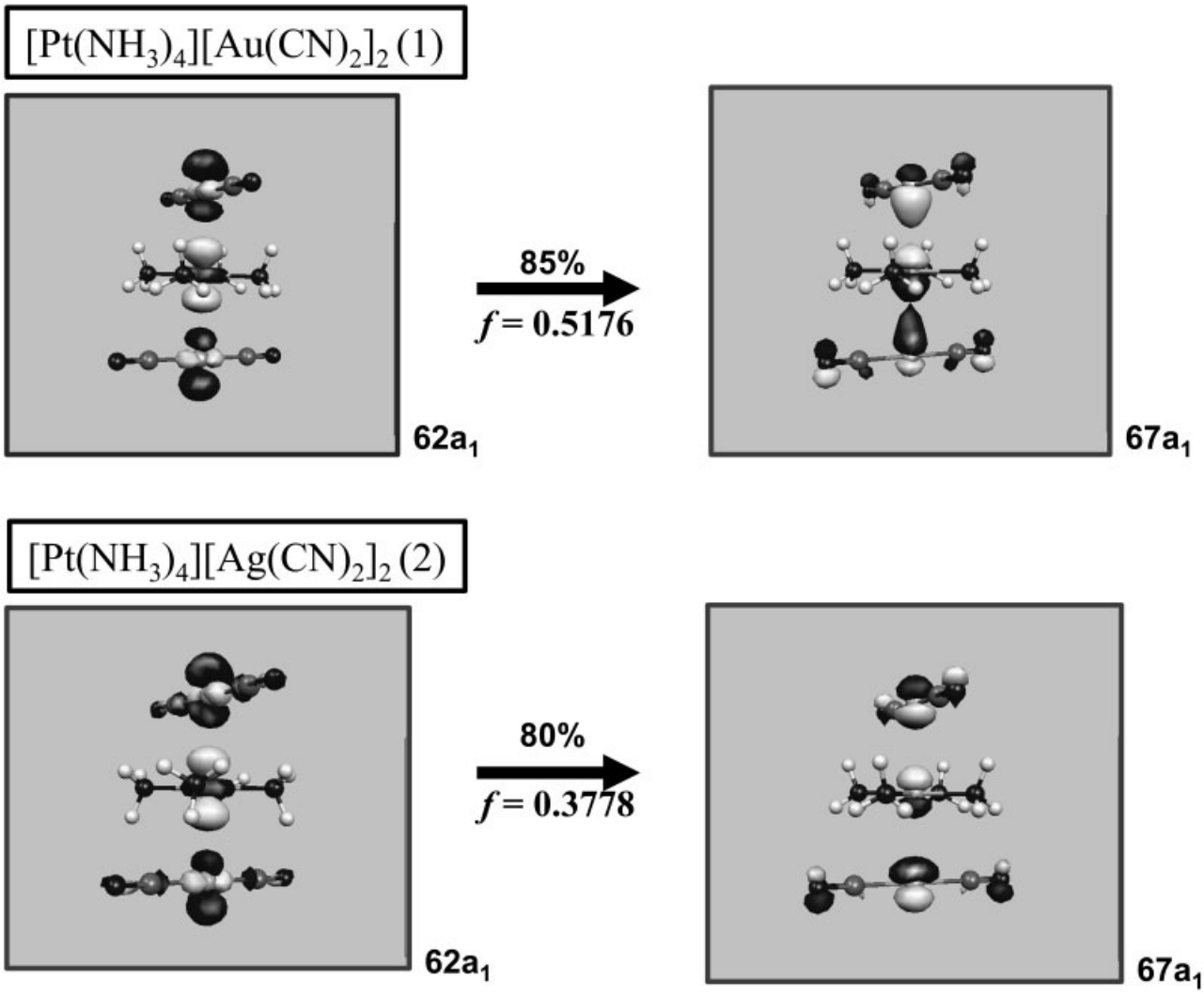

FIGURE 3. The molecular orbitals active in the principal electronic transition for $[Pt(NH_3)_4][Au(CN)_2]_2$ (**1**) and $[Pt(NH_3)_4][Ag(CN)_2]_2$ (**2**) at the PBE level.

transitions at 313 (**1**) and 304 nm (**2**) are caused mainly by $62a_1$ (dz^2) $\rightarrow$ $67a_1$ ($p\sigma$). This band corresponds to MMCT. The active molecular orbitals in the electronic transition are shown in Figure 3.

Also, Table IV describes the TD-HF and TD-B3LYP excitation for the same models. In qualitative terms, they are practically the same as in the analysis made with the PBE methodology (not shown here).

$[Pt(CNCH_3)_4][Pt(CN)_4]$ (M = Pt and Pd) (3, 4)

The theoretical transitions of the model systems (**3**, **4**) and experimental spectroscopic absorption data are summarized in Figure 2 and Table IV. The experimental spectra show intense absorption bands at 593 nm (**3**) and 437 nm (**4**), respectively [27]. In both complexes the electronic transition is assigned to $^1(d_{z2}(\sigma^*) \rightarrow p)$ [14].

The calculated spectra show a theoretical transition at 440 nm (**3**) and 441 nm (**4**), respectively. This transition is assigned to $68a_1 \rightarrow 69a_1$, HOMO-LUMO, at the PBE level, in agreement with the experimental one. This band corresponds to a metal-to-metal and ligand charge transfer (MMLCT)[1] ($d\sigma^* \rightarrow \pi^*$). The active molecular orbitals in the electronic transition are shown in Figure 4. The results with TD-HF and TD-B3LYP excitation are qualitatively the same as in the analysis made with the PBE methodology.

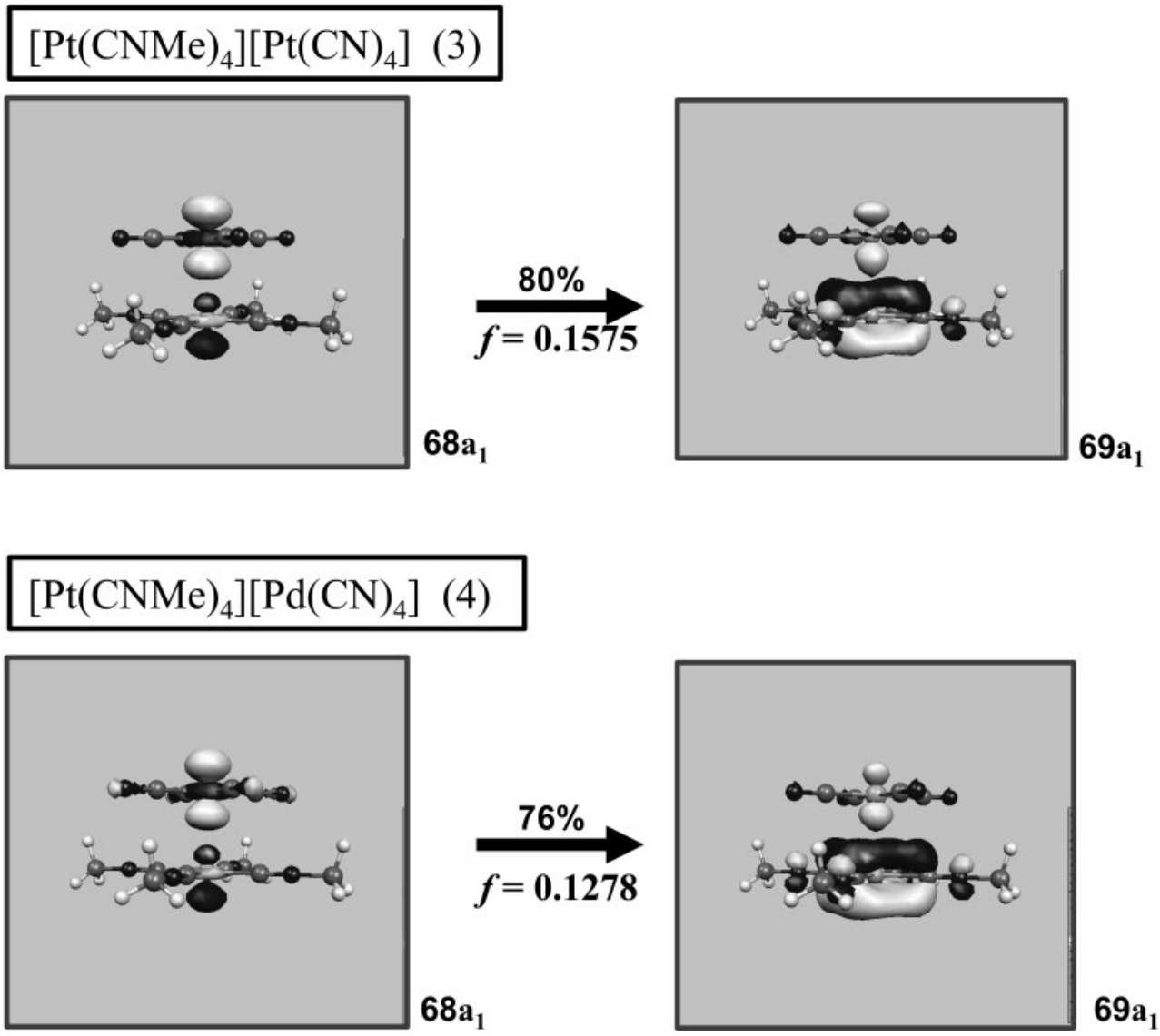

FIGURE 4. The molecular orbitals active in the principal electronic transition for $[Pt(CNCH_3)_4][Pt(CN)_4]$ (**3**) and $[Pt(CNCH_3)_4][Pd(CN)_4]$ (**4**) at the PBE level.

Conclusion

This study provides further information on the nature of the heteronuclear platinum-metal intermolecular interactions in the group complexes and their spectroscopic properties. Theoretical calculations at the MP2 level are in agreement with metallophilic attraction. On the other hand, TD-DFT/PBE calculations clearly match the experimental excitation spectra. They show that intermetallic interactions are mainly responsible for the MMCT in Models **1** and **2**, while Models **3** and **4** present a strong MMLCT component. For all models there is a strong dependency between the metal–metal intermolecular contact in each system and the MMCT or MMLCT band, with a red shift effect that is seen in the experimental solid state level.

References

1. Pyykkö, P. Chem Rev 1997, 97, 597.
2. Schmidbaur, H. Gold Bull 2000, 33, 1.
3. Gade, L. H. Angew Chem Int Ed Engl 1997, 36, 1171.

4. Mendizabal, F.; Zapata-Torres, G.; Olea-Azar, C. Chem Phys Lett 2005, 412, 477.
5. Mendizabal, F.; Olea-Azar, C. Int J Quantum Chem 2005, 103, 34.
6. Crespo, O.; Fernández, E. J.; Jones, P. G.; Laguna, A.; López-de-Luzuriaga, J. M.; Mendía, A.; Monge, M.; Olmos, M. E. Chem Commun 1998, 2233.
7. Crespo, O.; Laguna, A.; Fernández, E. J.; López-de-Luzuriaga, J. M.; Jones, P. G.; Teichert, M.; Monge, M.; Pyykkö, P.; Runeberg, N.; Schütz, M.; Werner, H.-J. Inorg Chem 2000, 39, 4786.
8. Pyykkö, P.; Runeberg, N.; Mendizabal, F. Chem Eur J 1997, 3, 1451.
9. Fernández, E. J.; Laguna, A.; López-de-Luzuriaga, J. M.; Monge, M.; Montiel, M.; Olmos, M. E. Inorg Chem 2007, 46, 2953.
10. Bardají, M.; Laguna, A. Eur J Inorg Chem 2003, 3069.
11. Fernández, E. J.; Jones, P. G.; Laguna, A.; López-de-Luzuriaga, J. M.; Mendizabal, F.; Monge, M.; Olmos, M. E.; Pérez, J. Chem Eur J 2003, 9, 456.
12. Fernández, E. J.; Jones, P. G.; Laguna, A.; López-de-Luzuriaga, J. M.; Monge, M.; Olmos, M. E.; Pérez, J. Inorg Chem 2002, 41, 1056.
13. Stender, M.; White-Morris, L.; Olmstead, M. M.; Balch, A. L. Inorg Chem 2003, 42, 4504.
14. Buss, C. E.; Anderson, C. E.; Pomije, M. K.; Lutz, C. M.; Britton, D.; Mann, K. R. J Am Chem Soc 1998, 120, 7783.
15. Pan, Q.-J.; Zhang, H.-X. Eur J Inorg Chem 2003, 4202.
16. Fernández, E. J.; Gimeno, M. C.; Laguna, A.; López-deLuzuriaga, J. M.; Monge, M.; Pyykkö, P.; Sundholm, D. J Am Chem Soc 2000, 122, 7287.
17. Barone, V.; Fabrizi de Biani, F.; Ruiz, E.; Sieklucka, B. J Am Chem Soc 2001, 123, 10742.
18. Mendizabal, F.; Olea-Azar, C.; Briones, R. Theochem 2006, 764, 187.
19. Perdew, J. P.; Burke, K.; Ernzerhof, M. Phys Rev Lett 1996, 77, 3865.
20. Bauernschmitt, R.; Ahlrichs, R. Chem Phys Lett 1996, 256, 454.
21. Olsen, L.; Jorgensen, P. In Modern Electronic Structure Theory; Yarkony, D. R., Ed.; World Scientific: River Edge, NJ, 1995; Vol. 2, p. 256.
22. Frisch, M. J.; Trucks, G. W.; Schlegel, H. B.; Gill, P. M. W.; Johnson, B. G.; Robb, M. A.; Cheeseman, J. R.; Keith, K. T.; Petersson, G. A.; Montgomery, J. A.; Raghavachari, K.; Al-Laham, M. A.;. Zakrzewski, V. G.; Ortiz, J. V.; Foresman, J. B.; Cioslowski, J.; Stefanov, B. B.; Nanayakkara, A.; Challacombe, M.; Peng, C. Y.; Ayala, P. Y.; Chen, W.; Wong, M. W.; Andres, J. L.; Replogle, E. S.; Gomperts, R.; Martin, R. L.; Fox, D. J.; Binkley, J. S.; Defrees, D. J.; Baker, J.; Stewart, J. P.; Head-Gordon, M.; Gonzalez, C.; Pople, J. A. Gaussian 03; Gaussian Inc.: Pittsburgh, PA.
23. Andrae, D.; Häusserman, U.; Dolg, M.; Stoll, H.; Preuss, H. Theor Chim Acta 1990, 77, 123.
24. Bergner, A.; Dolg, M.; Küchle, W.; Stoll, H.; Preuss, H. Mol Phys 1993, 80, 1431.
25. Huzinaga, S. J Chem Phys 1965, 42, 1293.
26. Mendizabal, F.; Aguilera, B.; Olea-Azar, C. Chem Phys Lett 2007, 447, 345.
27. Daws, C. A.; Exstrom, C. L.; Sowa, J. R.; Mann, K. R. Chem Mater 1997, 9, 363.